Spectroscopic Studies of the Modification of Crystalline Si(111) Surfaces with Covalently-Attached Alkyl Chains Using a Chlorination/Alkylation Method

Ashish Bansal,[†] Xiuling Li,[†] Sang I. Yi,[‡] W. H. Weinberg,*[,‡] and Nathan S. Lewis*[,†]

Division of Chemistry and Chemical Engineering, Noyes Laboratory, 127−72, California Institute of Technology, Pasadena, California 91125 and Department of Chemical Engineering, University of California, Santa Barbara, California 93106

Received: January 24, 2001; In Final Form: May 23, 2001

A two-step procedure, involving radical-initiated chlorination of the Si surface with PCl_5 followed by reaction of the chlorinated surface with alkyl-Grignard or alkyl-lithium reagents, has been developed to functionalize crystalline (111)-oriented H-terminated Si surfaces. The surface chemistry that accompanies these reaction steps has been investigated using X-ray photoelectron spectroscopy (XPS), Auger electron spectroscopy (AES), temperature programmed desorption spectroscopy (TPDS), high-resolution electron energy loss spectroscopy (HREELS), infrared (IR) spectroscopy in both glancing transmission (TIR) and attenuated total multiple internal reflection (ATR) modes, ellipsometry, and contact angle goniometry. The XPS data show the appearance of the Cl signal after exposure to PCl_5 and show its removal, and concomitant appearance of a C 1s signal, after the alkylation step. Auger electron spectra, in combination with TPD spectroscopy, demonstrate the presence of Cl after the chlorination process and its subsequent loss after thermal desorption of Si−Cl fragments due to heating the Si surface to 1200 K. High-resolution XP spectra of the Si 2p region show a peak corresponding to Si−Cl bond formation after the chlorination step, and show the subsequent disappearance of this peak after the alkylation step. IR spectra show the loss of the perpendicularly polarized silicon monohydride (Si−H) vibration at 2083 cm^{-1} after the chlorination step, whereas HREELS data show the appearance of vibrations due to Si−Cl stretches upon chlorination of the Si surface. The HREELS data furthermore show the disappearance of the Si−Cl stretch and the appearance of a Si−C vibration at 650 cm^{-1} after alkylation of the Si surface. Ellipsometric measurements indicate that the thickness of the alkyl overlayer varies monotonically with the length of the alkyl group used in the reactant. Contact angle and IR measurements indicate that the packing of alkyl groups in the monolayers produced by this method is less dense than that found in alkylthiol monolayers on Au. As determined by XPS, the alkylated surfaces show enhanced resistance to oxidation by various wet chemical treatments, compared to the H-terminated Si surface. The two-step reaction sequence thus provides a simple approach to functionalization of (111)-oriented, H-terminated silicon surfaces using wet chemical methods.

I. Introduction

The formation of monomolecular assemblies at solid surfaces provides a rational approach for fabricating interfaces having a well-defined composition, structure, and reactivity.[1−5] Despite the fact that the (100)- or (111)-oriented H-terminated silicon surfaces are the starting points for the construction of most contemporary electronic devices,[6] relatively little is known about the chemical reactivity of these crystalline Si surfaces under ambient temperature and pressure.[7−14] Control over the surface chemistry of Si is potentially important because the excellent physical and electrical properties of H-terminated Si surfaces are short-lived due to oxidation in air.[15] Functionalization of Si without partial oxidation and/or formation of electrical defects is therefore important in fabricating improved electronic devices[16,17] as well as in construction of stable Si-based photoelectrochemical cells for energy conversion purposes.[18,19]

Prior approaches to the functionalization of crystalline Si surfaces have mostly emphasized reactions of a thin silicon oxide layer that has been introduced onto the Si surface. The Si−OH bonds present on the surface of such systems have been exploited extensively through use of silanization reagents (such as chlorosilanes or alkoxysilanes), coupling reagents, and other related protocols that react with the surface silanols to produce covalently attached groups onto crystalline Si samples.[4,20−25] This chemistry is well-developed, and is closely analogous to the extensively documented protocols involved in controlling the surface chemistry of borosilicate glass or of oxide-containing chromatographic supports. However, this type of chemistry necessarily requires the presence of a thin oxide layer on the Si surface. This insulating silicon oxide not only introduces a tunneling barrier to interfacial charge transport, thereby affecting current flow in electrical devices,[16,26,27] but also generally introduces electrical trap sites and defects at the silicon/silicon oxide interface that can degrade the performance of electronic devices fabricated from such interfaces.[6,16]

Recent work has shown that well-defined monolayers of various reagents can be prepared on crystalline Si surfaces without first introducing a thin oxide overlayer onto the Si surface.[7−9,28−30] One such approach involves radical initiated reaction of Si−H bonds with olefins, forming hydrocarbon-based

* To whom correspondence should be addressed.
[†] Division of Chemistry and Chemical Engineering, Noyes Laboratory, California Institute of Technology.
[‡] Department of Chemical Engineering, University of California, Santa Barbara.

10.1021/jp010284p CCC: $20.00
Published on Web 10/03/2001

overlayers on the Si surface.[8,9] Another approach involves chlorination of the Si−H surface to yield a Si−Cl bond, followed by reaction with organolithium or Grignard reagents to yield an alkylated Si surface.[7,31,32] This paper focuses on the halogenation/alkylation reaction chemistry, which has been shown to preserve the excellent electrical properties of the H-terminated Si surface,[33] having an effective defect density of less than 1 electrical trap site per 10,000 surface atom sites. We present herein a detailed characterization of this reaction chemistry using surface science techniques involving ultrahigh-vacuum (UHV) and ambient atmospheres such as X-ray photoelectron spectroscopy (XPS), Auger electron spectroscopy (AES), temperature programmed desorption spectroscopy (TPDS), high-resolution electron energy loss spectroscopy (HREELS), infrared spectroscopy (IR) in glancing transmission (TIR) and attenuated internal reflection (ATR) modes, ellipsometry, contact angle goniometry, and surface stability. The data reported herein also relate to recent studies of the surface chemistry of porous Si[34−38] and thus provide a basis for a comparison of the reactivity of crystalline and porous Si surfaces with respect to various functionalization processes.

II. Experimental Section

A. Samples and Chemical Reagents. *1. Silicon Samples.* Samples used for XPS, HREELS, TPDS, and AES were phosphorus-doped, n-type, (111)-oriented, single-crystal Si wafers obtained from Wafernet Inc. These wafers were 100 mm in diameter and were polished to a smooth optical finish on the side that was used for spectroscopy. The samples were either 500 ± 50 μm thick, 1.5−3.0 ohm cm resistivity or were 575 ± 20 μm thick, 3−6 ohm cm resistivity. The single crystal (111)-oriented n-Si samples used in TIR spectroscopy experiments were 525 ± 25 μm thick, 24−34 ohm cm resistivity, 100 mm diameter wafers that were polished on both surfaces (Wacker Siltronic Corp.). For derivatization, samples of approximately 3 × 7 cm were cut from these double-polished wafers. Samples used for ATR experiments were 50 × 15 × 1 mm pieces of silicon (Harrick Scientific Corp.) in which the large parallel (50 × 15 mm) faces were (111)-oriented. Infrared light entered and exited the sample through the two small ends (15 × 1 mm), which made 45° angles with respect to the large parallel faces, producing 50 internal optical reflections of the incident beam.

2. Chemicals. Prior to use, anhydrous methanol (GR grade: EM Sciences) was dried under N_2(g) over powdered magnesium. Anhydrous tetrahydrofuran (THF) (GR grade: EM Sciences) was dried under N_2(g) over Na/benzophenone. Both solvents were distilled under N_2(g) from their respective drying agents into 500 mL flasks and were stored in a N_2(g)-purged glovebox prior to use. In some experiments, anhydrous THF obtained from Aldrich (in 800 mL sureseal bottles and stored in the N_2(g)-purged glovebox) was used in place of the distilled anhydrous THF described above. Dichloromethane (Omnisolve grade: EM Sciences) was used as received.

Phosphorus pentachloride (PCl_5), chlorobenzene, benzoyl peroxide, CH_3MgBr (3.0 M in diethyl ether), C_2H_5MgBr (3.0 M in diethyl ether), C_4H_9Li (2.5 M in hexanes), C_4H_9MgCl (2.0 M in diethyl ether), $C_5H_{11}MgBr$ (3.0 M in diethyl ether), C_6H_{13}-Li (2.0 M in hexane), $C_6H_{13}MgBr$ (2.0 M in diethyl ether), $C_8H_{17}MgCl$ (2.0 M in THF), $C_{10}H_{21}MgBr$ (1.0 M in diethyl ether), $C_{12}H_{25}MgBr$ (1.0 M in diethyl ether), and $C_{18}H_{37}MgCl$ (0.5 M in THF) were purchased from Aldrich and were used as received. $C_{10}H_{21}Li$ was prepared according to the method of Gilman et al.[39,40] $CF_3(CH_2)_3MgBr$ was prepared by reacting $CF_3(CH_2)_3Br$ (PCR Inc.) with Mg shavings.[39,40] CF_3CH_2OLi (0.77 M) was prepared by dissolving Li pieces in CF_3CH_2OH (Aldrich). The 40% NH_4F(aq) solution and a 5:1 (v:v) 40% NH_4F(aq)/49% HF(aq) solution (sold under the label "buffered hydrofluoric acid") were obtained from Transene Co. (Rowland, MA) and were used as received.

TABLE 1: XPS Data for Various Surface Treatments

−R	immersion time (h)	XPS C 1s/Si 2p ratio: expected[a]	survey	high resolution
−H				
$-CH_3$	10−14	0.09	0.32 ± 0.04	0.32 ± 0.01
$-C_2H_5$	2.5−10	0.09	0.30 ± 0.05	0.27 ± 0.04
$-C_4H_9$	2.5−8	0.20	0.48 ± 0.02	0.48 ± 0.02
$-C_5H_{11}$	16	0.26	0.70 ± 0.07	
$-C_6H_{13}$	5−18	0.31	0.66 ± 0.02	0.66 ± 0.01
$-C_8H_{17}$	16	0.43	0.66 ± 0.02	0.67
$-C_{10}H_{21}$	20−72	0.56	0.69 ± 0.08	0.72 ± 0.12
$-C_{12}H_{25}$	23−72	0.70	1.02 ± 0.07	1.05 ± 0.13
$-C_{18}H_{37}$	36−61	1.21	1.13 ± 0.09	1.09 ± 0.02

[a] Ratio calculated assuming all trans-conformation of alkyl chains packed onto 50% of the atop sites.

B. Surface Preparation. *1. Oxidation and Etching.* Prior to use, the silicon wafers were first cleaned by etching in aqueous 5:1 (v/v) NH_4F(aq):HF(aq) for 1−2 min followed by oxidation for 1 h in a 3:1 (v/v) solution of concentrated H_2SO_4:H_2O_2(aq) that was maintained at approximately 100 °C.[9] **Caution:** *The concentrated H_2SO_4:H_2O_2(aq) solution is very dangerous, particularly in contact with organic materials, and should be handled extremely carefully.* The samples were then removed from the acid solution, rinsed with copious amounts of water, dried at ∼80 °C, and stored for further use.

The oxidized silicon samples were etched in the 5:1 (v/v) NH_4F/HF(aq) solution for 30−60 s and then, without rinsing, were immersed into 40% NH_4F(aq) solution for 10−15 min.[41] The samples were subsequently removed from the NH_4F(aq), rinsed briefly with flash-photolyzed water and dried under a stream of N_2(g).

2. Chlorination. Chlorination of the silicon surface was carried out in a custom-built N_2(g)-purged glovebox that was connected via a load lock to the UHV system that housed the XP spectrometer. A stock chlorinating solution was prepared by dissolving enough PCl_5 in chlorobenzene to form a near-saturated solution (typically 0.6−0.7 M). Occasionally, the solution had to be heated at ∼60 °C for a few hours to achieve complete dissolution of the PCl_5. Immediately before use, a few grains of benzoyl peroxide (approximately 30−40 mg of benzoyl peroxide in 10 mL PCl_5/chlorobenzene solution) were added to a portion of the stock solution, the Si sample was immersed[42,43] and the solution was heated to 90−100 °C for 40−50 min. Subsequently, the sample was rinsed with anhydrous THF, rinsed with anhydrous methanol, and dried in a stream of N_2(g). After drying, the samples were mounted onto an XPS stub and were taken into the UHV chamber.

3. Alkylation. Alkylation of the chlorinated Si surfaces was also performed inside the N_2(g)-purged glovebox. In the alkylation step, the chlorinated Si(111) surfaces were immersed in alkyllithium (RLi: R = C_4H_9, C_6H_{13}, $C_{10}H_{21}$) or alkyl Grignard (RMgX: R = CH_3, C_2H_5, C_4H_9, $CF_3(CH_2)_3$, C_5H_{11}, C_6H_{13}, C_8H_{17}, $C_{10}H_{21}$, $C_{12}H_{25}$, $C_{18}H_{37}$; X = Br, Cl) solutions at 65−80 °C for 2−72 h.[39,44,45] The reaction time depended on the chain length of the alkyl group, with longer chains requiring longer times to achieve an apparent saturation of surface coverage (Table 1). After reaction, the samples were removed from solution, rinsed copiously with anhydrous THF, and then

TABLE 2: XPS Parameters Used in the Calculations of Various Coverages

		modified Scofield factors	
peak	binding energy (BeV)	survey scan	high-resolution scan
sensitivity exponent		0.65	0.60
F 1s	686	3.40	3.47
O 1s	532	2.52	2.55
C 1s	284.6	1.00	1.00
Cl 2s	270	1.70	1.70
Cl 2p	200	2.39	2.382
Si 2s	149	1.022	1.017
Si 2p	99	0.897	0.891

rinsed with anhydrous methanol. The samples were then immersed into a fresh portion of anhydrous methanol, taken out of the glovebox into air, and sonicated for 5 min, followed by sonication in dichloromethane for another 2−5 min. The samples were once again rinsed with methanol (EM Science: Omnisolve) and dried in a stream of air for 2−5 s before being taken into UHV for characterization by XPS.[46]

C. Surface Characterization Techniques. *1. X-ray Photoelectron Spectroscopy.* The XPS experiments were performed in an M-probe surface spectrometer (VG Instruments). Monochromatic Al Kα X-rays (1486.6 eV) incident at 35° from horizontal were used to excite electrons from the sample, and the emitted electrons were collected by a hemispherical analyzer at a takeoff angle of 35° from the plane of the sample surface (horizontal). The incident X-rays and the analyzer axis were in vertical planes that were at right angles to each other. All samples were sufficiently conducting that all reported energy measurements could be readily referenced to the Fermi level of the spectrometer.

Data collection and analysis (detailed in Supporting Information) were performed using the M-probe package software version 3.4. The "survey" scan was collected in the scanned mode with an 800 × 1500 μm elliptic spot. The "high resolution" scans were collected in an unscanned mode with the same spot size. The pass energies corresponding to the survey scan and the high-resolution scan were 154.97 and 53.98 eV, respectively. The corresponding energy windows in which the electrons were collected were 21.45 and 6.85 eV, respectively. The instrument had a resolution (full width at half-maximum (fwhm) for the Au $4f_{7/2}$ peak) of 1.50 ± 0.01 eV and 1.00 ± 0.01 eV, for the survey and high-resolution scans, respectively.

The Si 2p peaks in high resolution XP scans of the H-terminated and alkyl terminated surfaces were routinely deconvoluted into Si $2p_{1/2}$ and Si $2p_{3/2}$ components that represented primarily the "bulk" silicon atoms that resided within the sampling depth of the Si 2p XPS photoelectrons on the Si sample. For these surfaces, the chemical shifts of the surface silicon atoms bound to H or C were sufficiently small that any such surface Si peaks could not be resolved experimentally from the bulk Si peaks.[47−51] In the deconvolution procedure, the starting values for the fwhm for the nonoxidized Si 2p doublet peaks were typically adjusted to produce fits that minimized the difference between the fwhm values for the two best-fit peaks. Typically, this starting value difference was less than 0.02 eV. The overall spectra were best fit by using 95% Gaussian/5% Lorentzian line shapes with a 15% asymmetric contribution for each of the two component peaks.

For the chlorinated or the oxidized silicon surfaces, the chemical shift of the surface silicon atoms relative to the bulk silicon atoms was sufficiently large[52] that the contribution from the surface silicon atoms required introduction of a third peak component to obtain a good fit to the experimental XP spectrum. For these surfaces, deconvolution of the Si 2p doublet region for the nonoxidized peak was performed as described above.

The surface coverages of chlorine, fluorine, and alkyl groups on the silicon substrates were estimated using the XPS substrate-overlayer model.[53] The elemental sensitivity factors used in these calculations were modified Scofield factors,[54] and are given in Table 2.

The escape depth of Si 2p electrons through a Cl overlayer λ_{ov} (for the chlorinated surface) was taken to be equal to the attenuation length for Si 2p electrons through elemental Cl, as calculated using the empirical relationship[53]

$$\lambda = 0.41a^{1.5}E^{0.5} \quad (1)$$

where E is the electron kinetic energy in eV and λ and "a" are the attenuation length and thickness of a monolayer (in nm), respectively. The thickness of a monolayer of chlorine was calculated using the equation

$$A_{ov} = 1000D_{ov}N_{Av}a_{ov}^3 \quad (2)$$

where D_{ov} is the density of the overlayer (in kg m^{-3}), N_{Av} is Avogadro's number, a_{ov} is the thickness of the overlayer, and A_{ov} is the mean atomic weight of the atoms in the overlayer. The surface density of Cl atoms was taken to be equal to the density of liquid chlorine (1.5 g cm^{-3}).[55] Application of the above equations gave $a_{Cl} = 0.34$ nm. Using eq 1, the escape depths (λ_{ov}) through the Cl overlayer were calculated to be 2.9 nm for Cl 2p photoelectrons, 2.8 nm for Cl 2s photoelectrons, and 3.0 nm for Si 2p photoelectrons.

To calculate the coverage of chlorinated surface silicon atoms, Si_{Cl}, the high-resolution Si 2p spectrum was deconvoluted into three peaks. During deconvolution, the difference in the peak positions (0.6 eV), the peak area ratios (0.51), and the fwhm values of the $2p_{1/2}$ and $2p_{3/2}$ bulk components were held fixed.[56,57] A third peak (Si_{Cl}) was then added to the spectrum, and the positions of the three peaks and the width of the third peak were optimized to get the best fit to the experimental spectrum. Deconvolution using four peaks did not improve the fit to the experimental data. In accord with prior procedures,[58] the ratio of the Si_{Cl} peak to the sum of the Si $2p_{1/2}$ and $2p_{3/2}$ components, i.e., the ratio $Si_{Cl}/(Si\ 2p_{1/2} + Si\ 2p_{3/2})$, was used to calculate the coverage of chlorinated silicon atoms. The coverage of Si_{Cl} was then obtained through the method of Seah and Dench.[53] In this computation, the ratio of silicon atomic densities and sensitivity factors became unity and an escape depth value of $\lambda = 1.6$ nm was used for the substrate and for the overlayer.[47] The peak fitting for silicon samples covered with a thin layer of oxide was done similarly, with the third peak corresponding to the oxidized surface silicon atoms.

To determine the areal density of the alkyl overlayers obtained when the $CF_3(CH_2)_3MgBr$ or CF_3CH_2OLi reagents were used, the F 1s signal that originated from the $-CF_3$ groups was ratioed to the Si 2p signal of the substrate. The overlayer-substrate model was then applied to calculate the coverage of fluorine atoms on the surface. The overlayer thickness was calculated by assuming that the $-CF_3$ groups were at the solid-vacuum interface and that the $-CF_3$ groups were positioned at this location by the underlying methylene groups that were anchored rigidly to the silicon surface by covalent Si−C and Si−O bonds. This assumption was, however, not necessary to arrive at the coverage of alkyl chains (vide infra). An escape depth of $\lambda_{ov} =$ 2.65 nm was used for the F 1s signal and $\lambda_{ov} = 3.9$ nm was

used for the C 1s signal from the overlayer.[59] The escape depth of Si 2p electrons through the alkyl monolayer (λ_{sub}) was taken to be 3.5 nm.[47] The coverage of F atoms determined for surfaces derivatized with the two molecules was then divided by 3 to obtain the density of alkyl chains on the silicon surface. The alkyl chain density was then divided by the number of silicon atoms in the surface of the (111) plane to determine the effective alkyl coverage, in monolayers, on the Si surface.

2. High-Resolution Electron Energy Loss Spectroscopy. High-resolution electron energy loss spectroscopy (HREELS) measurements were carried out in a different UHV setup than the one used for the XPS measurements. The HREELS chamber was pumped by a 1000 L s^{-1} turbomolecular pump and was maintained at a base pressure of 7×10^{-11} Torr.[60] An external load lock and a UHV sample transfer system allowed fast loading of the samples into the chamber. The silicon specimens were mounted onto a molybdenum sample holder using two molybdenum tabs that were held in place with screws. The sample holder slid into a manipulator that was used for loading the samples into vacuum.

The HREELS measurements were performed on a model LK-2000−14-R spectrometer (LK Technologies). Data were collected at liquid nitrogen temperature (and sometimes at room temperature) in the direct mode at an angle of incidence of 60° with respect to the surface normal, with a primary beam energy of 7.5 eV and an energy resolution of 80 cm^{-1}. Off-specular measurements were made by moving the detector by a few degrees in a plane perpendicular to the surface plane of the Si sample.

3. Temperature Programmed Desorption. Temperature programmed desorption (TPD) data were obtained on the same samples and in the same UHV chamber that was used to obtain the HREELS data.[60] The samples were heated indirectly from the backside by resistively heated tungsten filaments, and a chromel−alumel thermocouple was spot-welded onto the central block that held the sample holder. An optical pyrometer and the desorption temperature of the mass 2 (H_2) peak from a Si(111) sample that had been sputtered with Ar^+-ions, thermally annealed and subsequently dosed with atomic hydrogen,[61] were used to calibrate the temperature scale of the thermocouple. The area under this mass 2 peak was used to estimate the signal intensity that represented a monolayer of hydrogen coverage. The TPD data were collected by ramping the temperature from 110 to 1200 K at a constant heating rate of either 0.5 K s^{-1} or 1 K s^{-1}. A differentially pumped quadrupole mass spectrometer (UTI-100C) with a cryoshroud was used to analyze the desorption products.

4. Auger Electron Spectroscopy (AES). Auger electron spectroscopic experiments were performed on the same samples and in the same UHV chamber as that used to collect the HREELS and TPD data. Auger data were collected with an electron energy of 3 keV using a PHI 10−155 single pass cylindrical mirror analyzer. The current on the crystal was ∼2 μA with an approximate beam size of 100 μm.

5. Infrared Spectroscopy. Infrared spectra (1 cm^{-1} resolution) were obtained using a Mattson Galaxy series (4326 upgrade) Polaris FT-IR spectrometer with external optics housed in a custom-built plexiglass chamber that was continuously purged with dry nitrogen. An InSb detector was used to probe the 4000−1800 cm^{-1} energy region and a mercury cadmium telluride detector was used to probe the 1800−800 cm^{-1} energy region. Glancing transmission (TIR) spectra were collected using large pieces of double-polished single-crystal Si(111) wafers, with the polarized infrared light incident onto the sample at Brewster's angle.

Absorption data for the H-terminated surface were obtained by ratioing the observed spectrum to that of the oxidized silicon sample. The absorption data for the chlorine-terminated or alkyl-terminated surfaces were obtained by ratioing these observed spectra to either the oxidized silicon sample or to the H-terminated sample. To determine the molecular orientation of the alkyl chains on the silicon surface, the infrared dichroic ratio, defined as the ratio of s-polarized to p-polarized absorption intensities ($D = A_{s-pol}/A_{p-pol}$), was determined for the symmetric (D_{sym}) and asymmetric (D_{asym}) methylene stretching peaks of the alkyl-terminated surfaces.[9] These dichroic ratios were then used to determine the angle between the surface normal and the dipole moments of the methylene symmetric and asymmetric stretches (α_{sym} and α_{asym}), respectively.[62] The chain tilt angle (θ) and twist angle (γ) were then calculated using eqs 3 and 4

$$\cos^2\theta = 1 - \cos^2\alpha_{sym} - \cos^2\alpha_{asym} \quad (3)$$

$$\cos\gamma = \frac{\cos\alpha_{sym}}{\sin\theta} \quad (4)$$

6. Ellipsometry. Ellipsometric measurements were made on a Gärtner Variable Angle L116C Ellipsometer using a He−Ne laser ($\lambda = 632.8$ nm), a 45° polarizer, and an incident angle of 70° from the surface normal. The optical constants $N_{Si} = 3.850$ and $K_{Si} = -0.020$, where N is the index of refraction, and K is the absorption coefficient, respectively, were used for the silicon substrate,[63] and values of $N_{ov} = 1.460$ and $K_{ov} = 0$ were used for the alkane films as well as for silicon oxide overlayers.[63] Ellipsometric data were collected at two or more spots per sample, with four or more measurements performed at each individual location. The ellipsometrically determined overlayer thicknesses were typically within ±0.2 nm on each sample and had a standard deviation of ±0.1 nm for a given spot on a sample. The errors in overlayer thickness produced by the assumption of $N_{Si} = 3.850$ and $K_{Si} = -0.020$ for the Si(111) substrate were determined to be ∼10% for a ±4% variation in N_{Si} and a 20% variation in K_{Si}.

7. Contact Angle Goniometry. Contact angles on alkyl-derivatized silicon surfaces were measured at ambient temperature and humidity using a Rame-Hart Inc. model 100−06 goniometer with a tiltable base. Flash photolyzed or 18 Mohm cm resistivity water obtained from a Barnstead water purification system was used for the experiments with aqueous drops, and anhydrous hexadecane (Aldrich) was used for nonaqueous drops. Prior to use, the hexadecane was passed through a column of activated basic alumina (Aldrich) that had been stored in the N_2(g)-purged glovebox. The sessile drop contact angle data were within ±2° for each drop and for each surface, with data collected generally on three drops per surface.

III. Results

A. The Hydrogen-Terminated Silicon Surface. NH_4F(aq)-etched, (111)-oriented Si surfaces were the starting point for our investigations. The Si atoms on such surfaces have been reported to be essentially completely terminated with hydrogen, forming Si−H bonds that are oriented normal to the (111) surface plane.[64−66] This passivated surface is also relatively chemically unreactive in atmospheric pressure ambients, including air[49] and, thus, provides a well-defined starting point for the systematic development of wet chemical functionalization procedures.

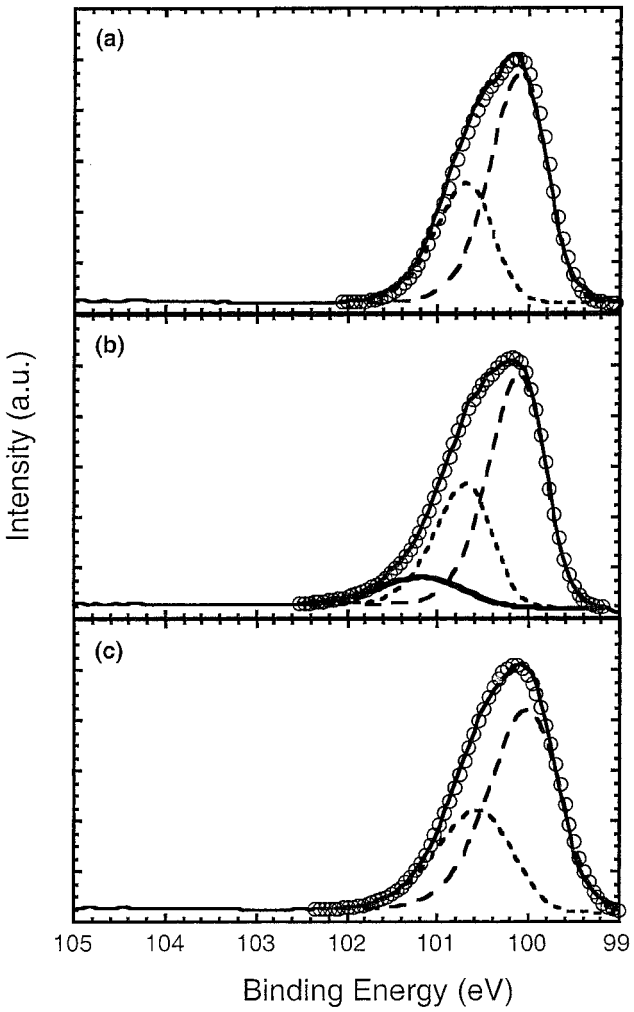

Figure 1. X-ray photoelectron "high resolution" spectra of the Si 2p region of a (111)-oriented Si surface after exposure to (a) 5:1 NH_4F-(aq)/HF(aq) to produce Si−H termination, (b) chlorination with PCl_5, and (c) alkylation with $C_6H_{13}Li$. The dashed lines are the fits to the Si 2p doublet peaks and the thick solid line in panel (b) is the additional peak needed at higher binding energy to obtain agreement between the actual data (upper solid line in each panel) and the fitted spectrum (open circles in each panel).

1. X-ray Photoelectron (XP) Survey Spectra. Typical XP survey spectra (provided in Supporting Information) of a H-terminated Si(111) sample contained two main peaks, at binding energies of 150.3 ± 0.2 eV and 99.0 ± 0.2 eV, respectively, which corresponded to signals expected from Si 2s and Si 2p photoelectrons.[47,48,67,68] Peaks observed at successive intervals of 17.5 eV higher than the two main peaks (i.e., at ∼116.5 BeV, 134.0 BeV, 167.5 BeV and 185.0 BeV) were characteristic of crystalline silicon samples and have been identified previously as plasmon loss peaks that arise from the Si 2s and 2p peaks.[69,70] Occasionally, small signals due to oxygen and carbon were also observed at 532 BeV (O 1s) and 284.6 BeV (C 1s), respectively, and are attributed to adventitious carbonaceous material present on the silicon surface as a result of wet chemical etching and subsequent brief handling of the surface in air (vide infra).[47,71] The lack of a F 1s signal in the XPS survey data, which would have appeared at ∼686 eV binding energy, confirmed that the NH_4F(aq)-etched silicon surface was not terminated by Si−F species at levels higher than 0.1 monolayer of F.[72,73]

2. High-Resolution XP Spectra. The high-resolution spectra of the Si 2p region (Figure 1a) could be deconvoluted into a doublet consisting of components from the $2p_{1/2}$ and $2p_{3/2}$ Si peaks.[47−49,67,68] Optimization of parameters of the two Si 2p component peaks to produce a best fit to the experimental spectrum yielded an average peak separation ($E_{Si\ 2p1/2} - E_{Si\ 2p3/2}$) of 0.60 ± 0.01 eV and an area ratio ($A_{Si\ 2p1/2}/A_{Si\ 2p3/2}$) of 0.51 ± 0.02. Both of these values are in excellent agreement with prior literature reports and with the theoretically expected values of 0.60 eV and 0.50, respectively.[47,48,67,68] After the deconvolution procedure, no statistically significant residual XPS signal was present in the Si 2p region, indicating negligible oxidation of the silicon surface, at least at the level of <0.2 monolayers that could be detected under these instrumental conditions.[47]

The lack of oxidized Si in the Si 2p region indicated that the O 1s and C 1s peaks observed in the survey scan at 532 BeV and 284.6 BeV, respectively, arose from adventitious species on the Si surface. These peaks could not always be completely eliminated during our etching and handling steps, which involved sample rinsing and transfer under ambient environment into the load lock of the UHV analysis chamber. Additional support for the hypothesis that the O 1s peak in the XPS survey scan was due to adventitious sources rather than from oxidation of the surface Si atoms was obtained from the empirical observation that the raw area ratio of the O 1s/C 1s peaks in the survey scan was observed to be 0.84 ± 0.15 for over 150 separate samples, whereas oxidation would have been expected to yield different O/C ratios for different oxidation levels. Even if all the oxygen observed in the survey scans were attributed to silicon oxide, the O 1s signal in the survey scan corresponds to <0.2 monolayer of oxide on the silicon surface.

3. Infrared Spectroscopy. Infrared spectra obtained with p-polarized light incident onto the NH_4F(aq) etched, (111)-oriented Si surface exhibited a sharp feature at 2083 cm^{-1} (spectra presented in Supporting Information). This peak position is indicative of the presence of surficial silicon monohydride species,[64−66] and the polarization anisotropy is consistent with the orientation of the transition dipole moment of the Si−H bond being normal to the Si (111) surface plane.[64] Small negative peaks observed in the C−H stretching region (2750−3000 cm^{-1}) indicated that the H-terminated surface had a lower amount of adventitious coverage than the reference (oxidized silicon) sample. Although on older Si ATR plates, whose surfaces had roughened somewhat due to repeated oxidation, etching and derivatization, some very small features indicative of $Si-H_2$ and $Si-H_3$ surface species were observed in the 2100−2140 cm^{-1} range, the glancing transmission IR spectra obtained on polished and freshly etched Si (111) wafers routinely showed no features above the noise in the 2100−2140 cm^{-1} region. Thus, silicon wafer surfaces were essentially completely terminated with Si−H species under the described conditions.

4. High-Resolution Electron Energy Loss Spectroscopy (HREELS) and Auger Electron Spectroscopy (AES). HREELS spectra obtained on H-terminated Si(111) surfaces (Figure 2a) exhibited peaks at 400 cm^{-1} (silicon bulk phonon modes), 800 cm^{-1} (CH_2 rocking mode), 1100 cm^{-1} (C−C stretching mode), 1400 cm^{-1} (CH_3 umbrella (wag) mode of the terminal methyl group) and 2950 cm^{-1} (C−H stretching mode).[74] The C−C and C−H HREELS peaks indicated the presence of some adventitious carbonaceous material on the surface. These observations are consistent with the XPS and AES results. Annealing these surfaces to 600 K lowered the hydrocarbon coverage somewhat but did not eliminate it completely. Due to the adventitious

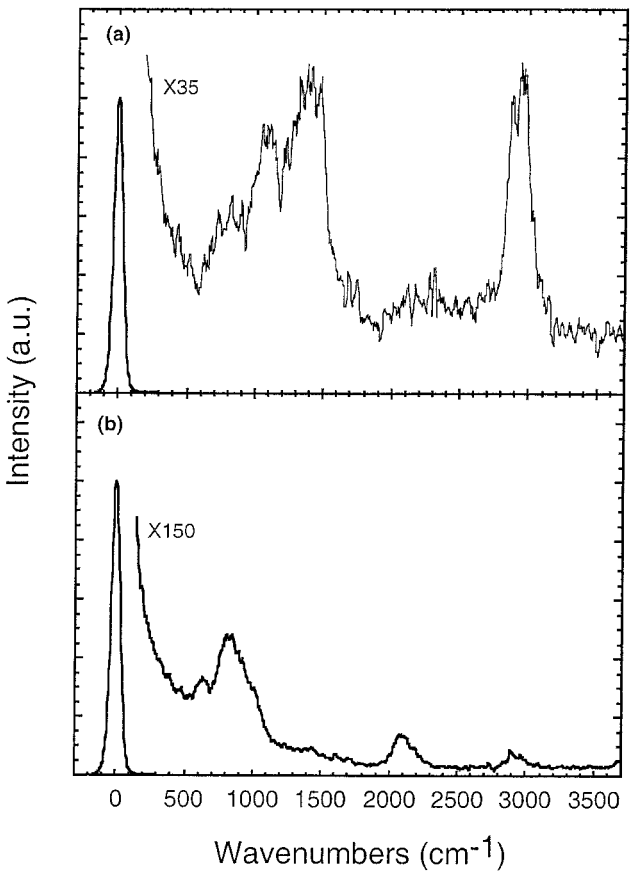

Figure 2. High-resolution electron energy loss spectra (HREELS) of a H-terminated Si(111) surface prepared by (a) etching in 5:1 NH_4F-(aq)/HF(aq) solution and 40% NH_4F(aq) solution and (b) dosing a Si-(111) surface, that had been previously sputtered with Ar^+ ions and annealed to 1200 K, with atomic hydrogen. The HREELS data were collected at a sample temperature of ~120 K.

carbonaceous overlayer, HREELS signals could not be observed for Si−H stretching peaks at ~2100 cm^{-1} for the etched Si samples.

In contrast, Si(111) samples that had been annealed in UHV to 1200 K and then exposed to atomic hydrogen did exhibit a distinct peak at ~2100 cm^{-1} (Figure 2b), verifying that the expected Si−H stretch could be observed for a clean hydrogen-terminated surface. These spectra also showed peaks at 650 and 850 cm^{-1}, corresponding to a Si−H bending mode and to the subsurface Si−C stretching mode, respectively.[60] For these samples, the 1100, 1400, and 2950 cm^{-1} peaks were either not observed or their intensity was extremely small. Although the HREELS signals were not very diagnostic for characterizing the wet-etched hydrogen terminated Si surfaces, these spectra serve as an important baseline for interpretation of the HREELS signals observed on chemically modified Si surfaces (vide infra).

Auger electron spectra of the NH_4F(aq)-etched (111)-oriented Si surface exhibited small carbon and oxygen KLL peaks at 272 and 503 eV, respectively, in addition to the Si LMM peak at 92 eV.[75,76] TPD spectra of such surfaces produced broad signals at masses 28 (C_2H_4), 27 (C_2H_3) and 2 (H_2) that were consistent with the presence of adventitious material on the surface.[61] AES spectra of samples that had been annealed to 1200 K and cooled to room temperature exhibited only the bulk silicon peak and did not exhibit carbon or oxygen Auger signals. When these samples were subsequently dosed with atomic hydrogen, sharp TPD peaks were observed for mass 2 at ~900 K. This desorption temperature is in accord with prior reports for the H-terminated, UHV prepared, Si (111) surface.[61]

B. The Chlorine-Terminated Si Surface. The H-terminated Si surface exhibited remarkable stability for a silane-type species, being relatively stable in air and water. In this regard, its chemistry resembled that of $((CH_3)_3Si)_3Si-H$, and stands in contrast to the reactivity of less hindered mono- or di-alkylsilanes such as $C_2H_5SiH_3$ or $(C_2H_5)_2SiH_2$. Difficulty in controlling the Si(111)−H surface chemistry was encountered when conventional hydrosilation methods were used because either no reaction was observed (with $Pt_2Cl_6^{2-}$ and olefins, [Rh-(COD)Cl]$_2$ and olefins, etc.) or extensive surface pitting, etching, and/or oxidation was observed when forcing conditions and highly reactive reagents (for example, high doses of Cl_2(g)) were used.

The H-terminated Si surface was, however, successfully chlorinated using PCl_5 in chlorobenzene, in a reaction that employed a mild source of chlorine radicals. The surface produced by this step could be manipulated under routinely available anaerobic laboratory conditions.

1. XP Survey Spectra. As compared to the H-terminated surface, the survey spectrum of the chlorine-terminated surface (shown in Supporting Information) displayed two additional peaks, at 270.2 ± 0.4 eV and 199.3 ± 0.4 eV binding energy, respectively, corresponding to signals arising from Cl 2s and Cl 2p photoelectrons.[76] The coverage of Cl on this surface was estimated to be 1.3−1.5 monolayers as determined from the ratio of the Cl 2s/Si 2p or Cl 2p/Si 2p peaks. None of the peaks changed in amplitude or position after sonication of the Si surfaces in anhydrous methanol or dichloromethane.

2. High-Resolution XP Spectra. Obtaining a satisfactory fit to the high-resolution Si 2p XPS data of the chlorinated surface (Figure 1b) required the use of three peaks. Two of these peaks corresponded to the $2p_{1/2}$ and $2p_{3/2}$ components of the bulk silicon doublet, as observed for the H-terminated surface, whereas the third peak, displaced toward higher binding energy, corresponded to surface silicon atoms that were bound to the chlorine atoms (Si_{Cl}). Optimization of the peak position and peak width of the high binding energy (Si_{Cl}) peak to give the best fit to the overall spectrum, whereas fixing the peak separation, peak area ratio and the fwhm of the $2p_{1/2}$ and $2p_{3/2}$ components to agree with those observed for the H-terminated Si surface, resulted in the Si_{Cl} peak being located at 1.09 ± 0.09 eV binding energy higher than the Si $2p_{3/2}$ component peak. This peak position is in excellent agreement with prior literature reports for Si(111) 7 × 7 surfaces that had been dosed with Cl_2(g) in UHV, in which a peak assigned to the $2p_{3/2}$ component of the surficial Si bonded to Cl was observed at 0.88−0.97 eV higher in energy than the Si $2p_{3/2}$ peak.[52,77] The coverage of chlorinated Si calculated from the ratio of the area of the Si_{Cl} peak to the Si 2p doublet was 0.66 ± 0.20 monolayers.

High-resolution XP spectra of the Cl 2p region were also collected for the chlorinated Si(111) surface between 197.4 and 204.2 eV binding energy. These spectra displayed a characteristic doublet of Cl $2p_{3/2}$ and Cl $2p_{1/2}$ peaks.[76] The ratio of the Cl 2p/Si 2p high-resolution peaks, both normalized for their data collection times and elemental sensitivity, gave a coverage of 1.3 ± 0.1 monolayers of chlorine on the silicon surface, consistent with the chlorine coverage determined from the XP survey spectra.

3. Infrared Spectroscopy. Infrared spectra of the chlorinated Si surface exhibited a complete loss of the Si−H stretch at 2083 cm^{-1} that was observed for the NH_4F(aq)-etched Si samples. This observation is consistent with the suggestion that the chlorination process converts the surface Si−H bonds to Si−Cl bonds. XP survey spectra of the chlorinated samples taken

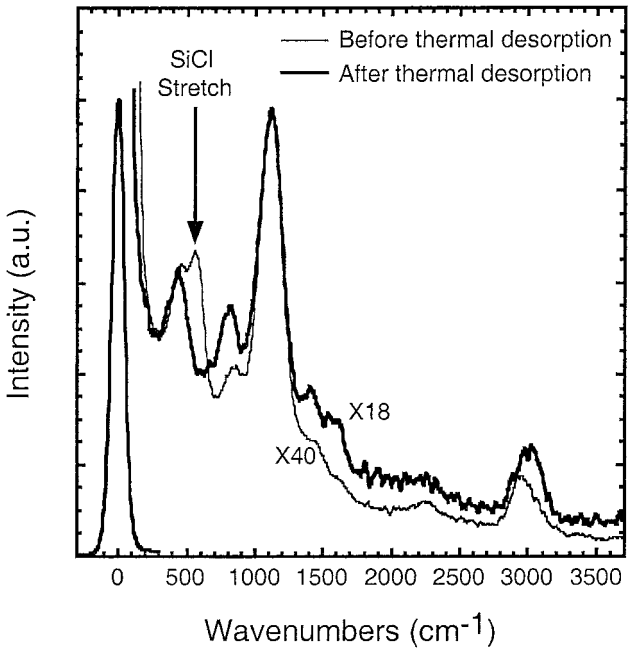

Figure 3. High-resolution electron energy loss spectra (HREELS) of a chlorine-terminated Si surface before (thin solid line) and after (thick solid line) thermal desorption to 1200 K. The peak at 550 cm^{-1}, present in the spectra before thermal desorption, corresponds to the Si−Cl stretching mode, and disappeared after thermal desorption of Cl.

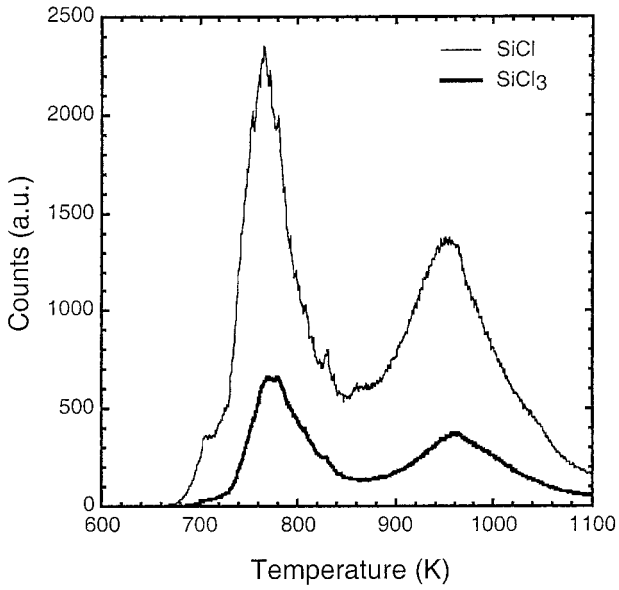

Figure 4. Temperature programmed desorption spectra of a chlorine-terminated Si surface. Peaks were observed at 63 amu (Si−Cl) and at 133 amu ($SiCl_3$).

before and after the IR measurements showed the same chlorine coverage on the surface, within experimental error. The high resolution XP spectra of the Si 2p region of these samples did not show any silicon oxide peak before or after IR measurement. These observations indicated negligible change in the nature of the chlorinated silicon samples during data collection or sample transfer. Concomitantly, no signatures were observed in the IR spectra that would indicate the presence of Si−O or Si−OH species on the chlorinated surface. The silicon−chlorine stretching mode that is expected to be produced by the chlorination step should appear at ∼550 cm^{-1}.[78] Unfortunately, this energy is not accessible in either conventional TIR or ATR geometries, due to strong absorption by bulk Si below 1500 cm^{-1}. Thus, no direct information on the presence of a Si−Cl bond could be obtained through the use of IR spectroscopy.

4. High-Resolution Electron Energy Loss Spectroscopy (HREELS). HREEL spectra of the Si−Cl surface exhibited a peak at 550 cm^{-1} (Figure 3) that was not present in the spectra for the Si−H surface. This peak position is in good agreement with prior reports of Si−Cl vibrations on chlorinated Si surfaces prepared in UHV[78] and is thus interpreted as confirming the formation of Si−Cl bonds on PCl_5-treated Si surfaces. After TPD to 1200 K, the 550 cm^{-1} peak due to surface Si−Cl was not observed in the HREEL spectra (Figure 3), in agreement with a lack of Cl signal in the Auger spectra after heating the sample to this temperature (vide infra).

5. Auger Electron Spectroscopy (AES) and Temperature Programmed Desorption (TPD). Auger/TPD data were used to confirm that the Cl observed in the Auger spectra was covalently bonded to the surface. Auger spectra taken on the chlorinated surface (shown in Supporting Information) exhibited a Cl LMM peak at 181 eV and small signals due to adventitious O and C at 503 and 272 eV, respectively, in addition to the bulk Si peak at 92 eV.[76] TPD spectra of the chlorine-terminated silicon surfaces (Figure 4) exhibited signals at mass 28, 27 and 2 that arose from adventitious adsorbed species (vide supra), but also exhibited signals at mass 63 (SiCl) and at mass 133 ($SiCl_3$) that were not observed on hydrogen-terminated Si surfaces prepared by dosing UHV-annealed Si surfaces with atomic hydrogen. These latter signals were consistent with the desorption of chlorinated species from the surface.[52,79] The observation of two peaks in the TPD signals for the chlorinated species suggested the formation of silicon di- and tri-chloride species in addition to silicon monochloride at the surface.

Auger spectra taken after heating the sample to 1200 K during the TPD experiment did not show any residual Cl AES signal. This demonstrates that all of the surficial Cl observed in the Auger spectrum of the chlorinated Si surface could be desorbed, and also demonstrates that the sample required a relatively high temperature in order to desorb most of the Cl from the surface. This set of observations suggests that all of the surface chlorine was covalently bound to the Si during the chlorination step, consistent with the HREELS data for this system.

C. Alkyl-Terminated Silicon Surfaces. The chlorinated Si(111) surfaces were found to react readily with organolithium and alkyl-Grignard reagents. To perform this derivatization step, the chlorinated silicon surfaces were immersed in alkyl Grignard (RMgX: R = CH_3, C_2H_5, C_4H_9, $(CH_2)_3CF_3$, C_5H_{11}, C_6H_{13}, C_8H_{17}, $C_{10}H_{21}$, $C_{12}H_{25}$, $C_{18}H_{37}$; X = Br, Cl) or alkyllithium (RLi: R = C_4H_9, C_6H_{13}, $C_{10}H_{21}$) solutions at 65−80 °C for various times (Table 1). The modified surfaces were spectroscopically and physically characterized as described below.

1. X-ray Photoelectron (XP) Survey Spectra. The XPS survey scan of the alkylated surfaces (shown for C_6H_{13}-terminated Si(111) in the Supporting Information) showed signals only due to Si, C and O. No Li or halide peaks were detected on such surfaces, and no Mg peaks were observed when $C_6H_{13}MgBr$ was used instead of $C_6H_{13}Li$ as the alkylation reagent. Furthermore, the C 1s/Si 2p ratio increased monotonically as the chain length of the alkyl group used to derivatize the sample was increased (Figure 5, Table 1).

2. High-Resolution XP Spectra. The high resolution XP spectra of the alkylated silicon surfaces were nearly identical to those obtained from H-terminated Si surfaces, and only required the use of Si $2p_{1/2}$ and Si $2p_{3/2}$ component peaks to obtain an excellent fit to the experimental data.[50] No significant residual was observed at high binding energy from the main

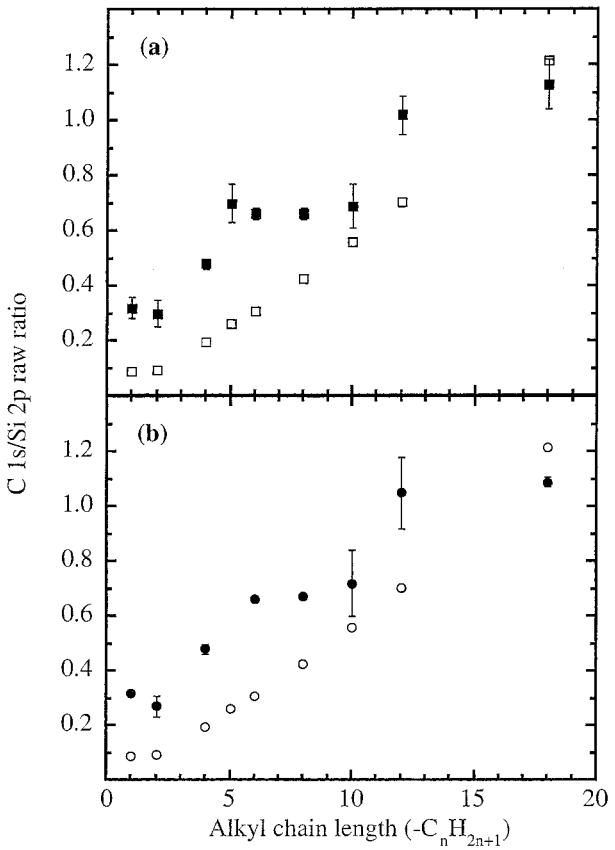

Figure 5. Observed and theoretically expected C 1s/Si 2p XPS peak ratios for silicon surfaces terminated with alkyl groups of different chain lengths in (a) survey XPS scans and (b) high resolution XPS scans. The solid squares denote the observed ratio and the open squares denote the expected ratio of C/Si peaks in the survey scan. The solid circles denote the observed ratio and the open circles denote the expected ratio of the C/Si peaks in the high resolution scan. The theoretically expected ratios for both scans were calculated for $-C_nH_{2n+1}$ ($2 \leq n \leq 18$) assuming 0.5 monolayer coverage (see text) and no contributions from adventitious carbonaceous material. For alkylation with $-CH_3$ groups, geometric factors permit the formation of one monolayer, and this coverage was assumed in the theoretical calculation for $n = 1$.

peak, indicating that the high binding energy Si 2p signal observed for the chlorinated surface had been removed during the alkylation step. Consistent with the very small intensity of the O 1s signal seen in the XP survey spectra, the high-resolution scans of the Si 2p region of alkylated surfaces showed no detectable oxidation of the surficial Si atoms. The lack of a chemical shift in the Si 2p region for the surficial Si atoms relative to the bulk Si atoms is consistent with expectations for Si−C bonding, in which the chemical shift of the surficial Si atoms is expected to be very close to that of lattice atoms involved in Si−Si bonding. The lack of oxidized Si signals is also consistent with the interpretation advanced above that the small O 1s signals observed in the XP survey scans are due to the presence of adventitious hydrocarbon species on such surfaces.

3. Infrared Spectroscopy. In the ATR mode of a $C_{12}H_{25}$-terminated surface, signals due to C−H stretching vibrations appeared at 2852 cm^{-1} ($\nu_s(CH_2)$), 2922 cm^{-1} ($\nu_a(CH_2)$), and 2961 cm^{-1} ($\nu_a(CH_3)$,ip) (shown in Supporting Information). No substantial signals were observed in the Si−H strecthing region. For the $C_{18}H_{37}$- and $C_{12}H_{25}$-terminated surfaces, ATR spectra yielded asymmetric methylene C−H stretching peaks at 2923 and 2922 cm^{-1}, respectively. These peak positions for alkylthiol

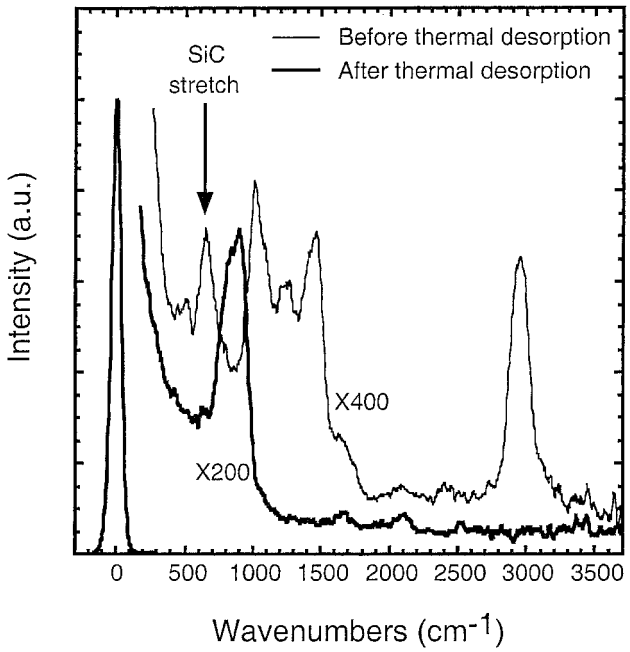

Figure 6. High-resolution electron energy loss spectra (HREELS) of an ethyl-terminated Si surface (made from exposing the chlorinated Si surface to C_2H_5MgBr) before (thin solid line) and after (thick solid line) thermal desorption to 1200 K. The peak at 650 cm^{-1}, present in the spectra before thermal desorption, corresponds to the Si−C stretching mode.

monolayers on gold have been interpreted to indicate a semi-amorphous environment of alkyl chains in the overlayer.[80,81]

Infrared dichroism measurements in the C−H stretching region[82] were used to estimate the average apparent tilt and twist angles of alkyl chains for Si surfaces that had been exposed to $C_{12}H_{25}MgBr$ or $C_{18}H_{37}MgBr$. Average α_{sym} and α_{asym} values were found to be 64° and 69° for the $-C_{12}H_{25}$ chains and 62° and 55° for the $-C_{18}H_{37}$ chains. Using eqs 3 and 4, the tilt and twist angles were determined to be 35° and 34°, respectively, for the $-C_{12}H_{25}$ chain and 48° and 51°, respectively, for the $-C_{18}H_{37}$ chain. The error in all the angles was estimated to be <3°. The tilt angles for the $C_{12}H_{25}$- and $C_{18}H_{37}$-terminated surfaces determined by IR spectroscopy were very close to those calculated from the ellipsometry data (vide infra).

4. High-Resolution Electron Energy Loss Spectroscopy (HREELS), Temperature Programmed Desorption Spectroscopy (TPDS) and Auger Electron Spectroscopy (AES). The Si−C stretching mode expected at ∼650 cm^{-1} [74,83,84] from a surficial Si-alkyl linkage cannot be observed by IR spectroscopy, in either TIR or ATR geometries, due to strong absorption by bulk Si below 1500 cm^{-1}. Chlorinated Si(111) surfaces that had been exposed to C_2H_5Li were therefore subjected to HREELS. As displayed in Figure 6, in addition to a peak for the C−H stretching mode at ∼2900 cm^{-1}, the CH_3 umbrella (wag) mode of the terminal methyl group at 1400 cm^{-1}, the C−C stretching mode at 1100 cm^{-1}, and the CH_2 rocking mode at 900 cm^{-1}, a strong signal was seen at ∼650 cm^{-1}.[74,83,84] The 650 cm^{-1} peak has been previously assigned to the Si−C stretching mode of alkylated Si(111) surfaces, based on vibrational analyses of adsorption of diethylsilane or ethylene on vacuum annealed Si-(111) surfaces in UHV.[74,83,84] In addition, Si−C stretches at similar energies have been identified in vibrational spectra of alkylated Si(100) surfaces that have been prepared by adsorption of acetylene or ethylene onto annealed Si(100) surfaces in UHV.[60,83] All of the vibrational peaks observed in the HREELS

spectra were either significantly reduced or disappeared completely after thermal desorption at 1200 K (Figure 6).

The Auger spectra were consistent with the HREELS data. Peaks in the Auger spectrum of a chlorinated Si surface that had been subsequently exposed to C_2H_5Li were observed for Si and C at 92 and 272 eV, respectively (spectra shown in Supporting Information). A trace amount of Cl was observed on the alkylated surface, as indicated by a small peak at 181 eV. All peaks except the bulk silicon signal disappeared after the sample was heated to ~1200 K and cooled to room temperature.

5. Estimates of the Coverage of Alkyl Overlayer Groups Derived from XPS. To estimate the areal coverage of alkyl species on the silicon surface, the chlorinated Si surface was derivatized with $CF_3(CH_2)_3MgBr$ or with CF_3CH_2OLi. Using F 1s/Si 2p ratios from the survey spectra, the overlayer−substrate model gave a coverage of 0.43 ± 0.05 monolayers for surfaces derivatized with $CF_3(CH_2)_3MgBr$ and 0.51 ± 0.01 monolayers for surfaces derivatized with CF_3CH_2OLi. In this method, the $-CF_3$ groups were assumed to be at the solid-vacuum interface, held there by the underlying methylene groups which were anchored rigidly to the silicon surface by covalent Si−C and Si−O bonds. If instead the chains were assumed to not be held rigidly but the F atoms were uniformly, but randomly, distributed in the overlayer, the coverage values obtained were 0.50 ± 0.06 and 0.57 ± 0.10 for the survey and high-resolution data, respectively, for surfaces treated with $CF_3(CH_2)_3MgBr$ and was 0.51 ± 0.01 from the survey data of surfaces exposed to CF_3CH_2OLi. Analysis of the ratio of the high-resolution peaks of F 1s and Si 2p signals for surfaces derivatized with $CF_3(CH_2)_3MgBr$ gave an alkyl coverage of 0.48 ± 0.09 monolayers. These coverages are consistent with the hypothesis that alkyl chains cannot be attached to every surface silicon atom, because the diameter of the alkyl chain (4.85 Å)[85] is larger than the 3.84 Å distance between adjacent atop sites of the unreconstructed Si(111) surface.[16]

The high-resolution Si 2p spectra for the CF_3CH_2OLi-exposed surfaces were also of interest in that they indicated the presence of peaks due to oxidized Si at 3.6 ± 0.1 eV higher than the Si $2p_{3/2}$ peak in an unoxidized Si overlayer. The coverage of oxidized Si atoms was calculated from the ratio of the area of the silicon oxide peak to the area of the bulk Si 2p doublet signal, and this calculation indicated a coverage of ~1.6 monolayer of oxidized Si on such surfaces.

XPS data were also used to estimate the variation in coverage as a function of the length of the alkyl chain in the overlayer. Figure 5 shows the C 1s/Si 2p ratio calculated from the survey scan and from high-resolution scans of alkylated Si surfaces (Si−R: R═C_nH_{2n+1}, $1 \le n \le 18$). Also shown, for comparison, are the corresponding C 1s/Si 2p ratios expected for a monolayer with uniform ideal coverage of a given chain length. The expected ratio for both the survey and high-resolution scans were calculated for $-C_nH_{2n+1}$ ($2 \le n \le 18$) assuming half-monolayer coverage and no contributions from adventitious C sources. For $n = 1$, geometric factors permit the formation of one monolayer, and this has been assumed in the calculation for methyl termination only.

Although some deviations are apparent between the observed and the ideally expected values, the data are in general agreement with expectations. The presence of adventitious carbon is expected to cause the observed ratio to be higher than the ideally expected value for all chain lengths. In contrast, a less than optimal density of the overlayer, due to either incomplete overlayer formation or significant tilt of the alkane chains, is expected to manifest itself as a decrease in the observed C 1s/Si 2p ratio as compared to the ideally expected value. The experimentally observed ratio contains both of these factors (perhaps in different proportions) for each chain length.

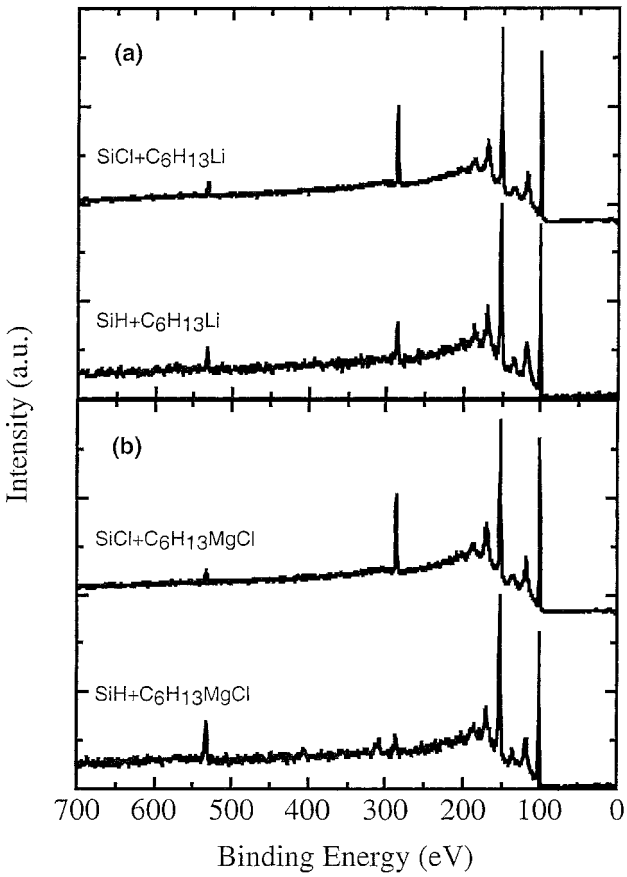

Figure 7. XPS survey spectra of a chlorine-terminated and hydrogen-terminated Si surface that were exposed to $C_6H_{13}MgBr$ and $C_6H_{13}Li$ reagents, respectively, for 6−10 h at 330 K.

6. Reactivity of the H−Terminated Si Surface Toward Alkylation Reagents. Figure 7 compares the XP survey spectra obtained when chlorinated and hydrogen-terminated crystalline (111)-oriented Si surfaces were reacted with $C_6H_{13}Li$ and $C_6H_{13}MgBr$, respectively. The C 1s/Si 2p peak ratio was always smaller when the H-terminated Si surface was used than when the Cl-terminated Si surface was used. The Li reagents produced a higher C 1s/Si 2p ratio under the same time and temperature conditions than was observed when the analogous Mg reagents were used. In some cases, the Mg reagent produced relatively little apparent alkylation, whereas in other cases somewhat higher C 1s/Si 2p ratios were observed. The less reactive behavior of the NH_4F(aq)-etched, H-terminated, (111)-oriented Si surface relative to the chlorinated Si(111) surface therefore underscores the advantage of the two-step procedure in obtaining a high coverage of surface functional groups, under the time and temperature conditions explored during the course of this work.

7. Ellipsometry. Ellipsometric measurements of the alkylated surfaces gave effective overlayer thicknesses that increased monotonically with the length of the alkane chain used in the reactant molecules (Figure 8; Table 3). The thicknesses obtained from analysis of the ellipsometric data were consistent with the C 1s/Si 2p ratios observed by XPS (Figure 5). The measured ellipsometric thicknesses for the alkyl monolayers made from reagents having from short ($n \le 6$) chains were consistently approximately 0.3 nm higher than the values calculated for the

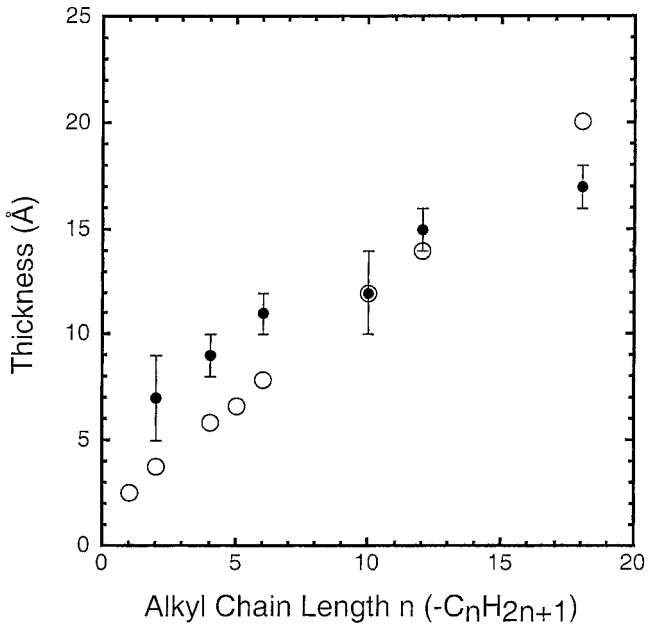

Figure 8. Ellipsometrically determined thicknesses of the monolayers prepared from alkyl groups of different chain lengths ($-C_nH_{2n+1}$: $1 \leq n \leq 18$). Solid circles denote the experimentally determined thicknesses, while the open circles denote the theoretically expected values based on a model that assumes that the alkane chains are in an all-trans configuration and are held rigidly by the underlying Si−C bonds. The model does not include any contributions from adventitious carbon to the thickness of the monolayers.

TABLE 3: Physical Properties of Alkyl-terminated Si(111) Surfaces

−R	observed ellipsometric thickness (Å)	calculated film thickness[a] (Å)	contact angle: water (°)	contact angle: hexadecane (°)
$-C_2H_5$	7 ± 2	3.82	85 ± 3	<10
$-C_4H_9$	9 ± 1	5.85	95 ± 2	<10
$-C_6H_{13}$	11 ± 1	7.89	100 ± 2	30 ± 1
$-C_{10}H_{21}$	12 ± 2	11.95	93 ± 2	<10
$-C_{12}H_{25}$	15 ± 1	13.98	104 ± 2	27 ± 1
$-C_{18}H_{37}$	17 ± 1	20.08	99 ± 2	37 ± 1

[a] The calculation assumes that the alkyl groups are rigidly bound to the surface of silicon and the Si−C bond is normal to the surface.

thickness of such chains in their all trans- conformation.[62,80,81] Consistent with XPS survey data and AES data, this difference is likely due to the presence of adventitious hydrocarbon species on the alkylated surface. Surfaces prepared from longer chain alkyl groups ($10 \leq n \leq 18$) showed variable differences between the ellipsometrically observed and theoretically expected values, likely due to varying contributions from adventitious carbon and packing-density-dependent chain tilts (vide supra). When the observed ellipsometric thicknesses for the $C_{12}H_{25}$- and $C_{18}H_{37}$-terminated surfaces were corrected for the contribution of adventitious carbon (assumed to be constant for the series of alkyl overlayers), and the residual thickness of the overlayer then compared with the calculated length of the respective molecule in the all trans- conformation, the average chain tilt angles were found to be 31° for the $C_{12}H_{25}$-terminated surface and 45° for the $C_{18}H_{37}$-terminated surface, in good agreement with the results from the IR dichroism measurements (vide supra).

8. Contact Angle Goniometry. Contact angle measurements were performed with water and hexadecane to gain additional information regarding the ordering of the free ends of the alkyl chains of the alkylated Si(111) surfaces. In studies involving alkylthiol monolayers on gold or involving alkyl monolayers prepared from radical addition of 1-alkenes onto (111)-oriented silicon, contact angles for water in the range 110°−115° and for hexadecane in the range 45°−50° have been taken to indicate a tightly packed alkyl monolayer with a free surface terminated by methyl groups. Lower contact angles in such systems have been interpreted to indicate the presence of exposed methylene groups at the surface.[8,9,80,81] Contact angle measurements on the alkyl-terminated Si surfaces gave angles between 85° and 105° for water and 36° or lower for hexadecane (Table 3). This suggests that the surface contained some amount of exposed methylene units at the surface. The methylene units could be exposed either due to a less than optimal packing density of the alkyl chains or due to significant tilting of the alkyl chains from surface normal. Either of these scenarios is consistent with the infrared data, which indicate a semi-amorphous packing in the monolayer. This observation is also consistent with the half-monolayer packing density that was determined from analysis of the XPS data (vide supra).

9. Chemical Stability of the Alkylated Si Surfaces. It is of interest to probe whether surface alkylation results in enhanced stability to oxidation, as might be expected if Si−H bonds have been replaced by Si−C bonds. A hydrogen-terminated surface and a representative alkylated Si surface, derivatized with C_4H_9-Li (after chlorination of the Si) were therefore immersed for 30 min in boiling aerated chloroform. After immersion, the C 1s/Si 2p peak ratio in the XPS survey scan retained 90% of its original intensity, and no oxidation was observed by XPS for either the H-terminated surface or the alkyl-terminated surface under such conditions.

XPS analysis of two $C_{12}H_{25}$-terminated silicon samples that had been exposed to aqueous H_2SO_4(aq) (pH = 2) and KOH (pH = 13) solutions, respectively, for 2.5 h at room temperature produced almost no change in the carbon coverage in XPS survey scans of the surface. In contrast, the H-terminated Si surface showed approximately one monolayer of oxide coverage after being subjected to the same conditions. Similarly, approximately one monolayer of oxide was observed on the H-terminated surface after exposure to the basic solution, whereas only ~0.5 monolayers of oxide were observed by XPS on the $C_{12}H_{25}$-terminated surface.

The stability of the alkyl-terminated surfaces toward HF(aq) was measured by immersing a $C_{10}H_{21}$-terminated Si(111) sample into a 5:1 (v:v) NH_4F(aq)/HF(aq) solution for 5 min. XP spectra of the surface taken before and after immersion showed no significant change in the C 1s/Si 2p ratio. Furthermore, when a $CF_3(CH_2)_3$-terminated sample that exhibited ~0.5 monolayer of silicon oxide was immersed for 5 min into the 5:1 (v:v) NH_4F(aq)/HF(aq) solution, subsequent analysis by XPS revealed that the F 1s/Si 2p ratio had retained 82% of its original intensity. Furthermore, no silicon oxide was observed on the $CF_3(CH_2)_3$-terminated surface after the etch. These results indicate that the alkyl groups are primarily attached directly to the silicon surface and not through an intervening oxide layer, and that the oxide but not the alkylated Si, had been etched by the fluoride-containing solutions.

IV. Discussion

The two-step reaction sequence described above, radical-initiated chlorination followed by reaction with Grignard or organolithium reagents, provides a simple, apparently general approach to functionalization of H-terminated silicon surfaces. Moreover, this procedure allows the formation of important

surface functionalities, such as the methyl-terminated Si surface, that are not readily available through many other routes. The alkyl overlayers are robust and impart enhanced chemical stability to the silicon surface in the presence of a variety of oxidizing ambients. This behavior might be especially important in the uses of these surfaces for electrical devices because protection against inadvertent interfacial oxidation is a critical feature for many applications of Si surfaces.

The contact angle, ellipsometric, and other physical data on these alkylated Si surfaces are consistent with the hypothesis that the packing of chains in these alkyl overlayers is less dense than that displayed by alkylthiols on Au. The van der Waals radius of a methylene unit is sufficiently large that packing an alkyl chain onto every Si atom is expected to be highly unfavorable sterically.[85] This expectation compares favorably with the ~0.5 monolayer coverage determined from XPS measurements on fluorine-tagged alkyl overlayers.[86]

The present study also reveals significant differences in reactivity between porous Si surfaces and crystalline Si surfaces. Recent work has demonstrated both halogenation and alkylation of porous Si surfaces.[37] Partial alkylation has been reported upon direct exposure of H-terminated porous Si surfaces to Grignard or organolithium reagents, presumably through attack on the Si−Si back-bonds.[37] Partial alkylation was also observed using such methods on the crystalline Si surfaces investigated in our study. Halogenation treatments of porous Si are reported to produce preferential reaction with di- and tri-hydride Si species, whereas only a fraction of the monohydridic Si−H bonds on such surfaces are reactive.[34−36,38] In contrast, the reactions described herein produced a complete disappearance of the Si−H bonds on crystalline, (111)-oriented, Si surfaces. These differences imply the presence of a distribution of Si−H sites, having varying degrees of reactivity, on porous Si surfaces as compared to the reactivity of the Si−H bonds on crystalline, H-terminated (111)-oriented Si surfaces. A detailed comparison between the reactivity of porous Si and crystalline Si toward several types of reagents would be of interest to define further the degree to which the Si−H bonds on these different surfaces share a common reaction chemistry.

V. Conclusions

Radical-initiated chlorination of crystalline (111)-oriented Si surfaces with PCl_5, followed by reaction of the chlorinated surface with alkyl-Grignard or alkyl-lithium reagents, produces alkylated Si surfaces that show enhanced resistance to oxidation by various wet chemical treatments as compared to the H-terminated Si surface. XPS and ellipsometric measurements indicate that the thickness of the alkyl overlayer varies monotonically with the length of the alkyl group used in the reactant, whereas contact angle and IR measurements indicate that the packing of alkyl groups in the monolayers produced by this method is less dense than that found in alkylthiol monolayers on Au.

Acknowledgment. We acknowledge the NSF, Grant No. CHE-997456, for support of this work. Si wafers polished on both sides were generously provided by Mr. Daniel L. McDonald of Wacker Siltronic Corp. We also acknowledge Dr. Steve Doig for constructing the surface IR apparatus and Dr. Alan Rice for assistance with, and technical support of, the UHV equipment.

Supporting Information Available: Surface Characterizations by X-ray Photoelectron Spectroscopy. This material is available free of charge via the Internet at http://pubs.acs.org.

References and Notes

(1) Ulman, A. *An Introduction to Ultrathin Organic Films*; Academic: San Diego, CA, 1991.
(2) Leyden, D. E.; Collinus, W. *Silylated Surfaces*; Gordon and Breach, Science Publishers Inc.: New York, 1980.
(3) *Silanes, Surfaces, and Interfaces*; Leyden, D. E., Ed.; Gordon, Breach and Harwood: Snowmass, Colorado, 1986; Vol. 1.
(4) Calvert, J. M. *Organic Thin Films and Surfaces*; Academic Press: San Diego, CA, 1993.
(5) Roberts, G. *Langmuir−Blodgett Films*; Plenum Press: New York, 1990.
(6) Wolf, S.; Tauber, R. N. *Silicon Processing for the VLSI Era*; Lattice Press: Sunset Beach, 1986.
(7) Bansal, A.; Li, X.; Lauermann, I.; Lewis, N. S.; Yi, S. I.; Weinberg, W. H. *J. Am. Chem. Soc.* **1996**, *118*, 7225−7226.
(8) Linford, M. R.; Chidsey, C. E. D. *J. Am. Chem. Soc.* **1993**, *115*, 12 631−12 632.
(9) Linford, M. R.; Fenter, P.; Eisenberger, P. M.; Chidsey, C. E. D. *J. Am. Chem. Soc.* **1995**, *117*, 3145−3155.
(10) Lauerhaas, J. M.; Sailor, M. J. *Science* **1993**, *261*, 1567−1568.
(11) Lee, E. J.; Ha, J. S.; Sailor, M. J. *J. Am. Chem. Soc.* **1995**, *117*, 8295−8296.
(12) Allongue, P.; Kieling, V.; Gerischer, H. *J. Phys. Chem.* **1995**, *99*, 9472−9478.
(13) Ando, A.; Miki, K.; Matsumoto, K.; Shimizu, T.; Morita, Y.; Tokumoto, H. *Jpn. J. Appl. Phys.* **1996**, *35*, 1064−1068.
(14) Lei, J. A.; Bai, Y. B.; Wang, D. J.; Li, T. J.; Tian, K. E. *Thin Solid Films* **1994**, *243*, 459−462.
(15) Hsu, J. W. P.; Bahr, C. C.; vom Felde, A.; Downey, S. W.; Higashi, G. S.; Cardillo, M. J. *J. Appl. Phys.* **1992**, *71*, 4983−4990.
(16) Sze, S. M. *The Physics of Semiconductor Devices*, 2nd ed.; Wiley: New York, 1981.
(17) Buczkowski, A.; Radzimski, Z. J.; Rozgonyi, G. A.; Shimura, F. *J. Appl. Phys.* **1991**, *69*, 6495.
(18) Lewis, N. S. *Annu. Rev. Phys. Chem.* **1991**, *42*, 543−580.
(19) Tan, M. X.; Laibinis, P. E.; Nguyen, S. T.; Kesselman, J. M.; Stanton, C. E.; Lewis, N. S. *Prog. Inorg. Chem.* **1994**, *41*, 21−144.
(20) Wasserman, S. R.; Tao, Y. T.; Whitesides, G. M. *Langmuir* **1989**, *5*, 1074−1087.
(21) Wasserman, S. R.; Whitesides, G. M.; Tidswell, I. M.; Ocko, B. M.; Pershan, P. S.; Axe, J. D. *J. Am. Chem. Soc.* **1989**, *111*, 5852−5861.
(22) Maoz, R.; Sagiv, J. *J. Colloid Interface Sci.* **1984**, *100*, 465−496.
(23) Pomerantz, M.; Segmuller, A.; Netzer, L.; Sagiv, J. *Thin Solid Films* **1985**, *132*, 153−162.
(24) Dulcey, C. S.; Georger, J. H.; Krauthamer, V.; Fare, T. L.; Stenger, D. A.; Calvert, J. M. *Science* **1991**, *252*, 551.
(25) Silberzan, P.; Leger, L.; Aussere, D.; Benattar, J. J. *Langmuir* **1991**, *7*, 1647.
(26) Kumar, A.; Rosenblum, M. D.; Gilmore, D. L.; Tufts, B. J.; Rosenbluth, M. L.; Lewis, N. S. *Appl. Phys. Lett.* **1990**, *56*, 1919−21.
(27) Fonash, S. J. *Solar Cell Device Physics*; Academic: New York, 1981.
(28) Allongue, P.; Henry de Villeneuve, C.; Pinson, J.; Ozanam, F.; Chazalviel, J. N.; Wallart, X. *Electrochim. Acta* **1998**, *43*, 2791−2798.
(29) Henry de Villeneuve, C.; Pinson, J.; Ozanam, F.; Chazalviel, J. N.; Allongue, P. *Mater. Res. Soc. Symp. Proc.* **1997**, *451*, 185−195.
(30) He, J.; Patitsas, S. N.; Preston, K. F.; Wolkow, R. A.; Wayner, D. D. M. *Chem. Phys. Lett.* **1998**, *286*, 508−514.
(31) Bansal, A.; Lewis, N. S. *J. Phys. Chem. B* **1998**, *102*, 4058−4060.
(32) Bansal, A.; Lewis, N. S. *J. Phys. Chem. B* **1998**, *102*, 1067−1070.
(33) Royea, W. J.; Juang, A.; Lewis, N. S. *Appl. Phys. Lett.* **2000**, *77*, 1988−1990.
(34) Buriak, J. M.; Allen, M. J. *J. Am. Chem. Soc.* **1998**, *120*, 1339−1340.
(35) Lee, E. J.; Ha, J. S.; Sailor, M. J. *Mater. Res. Soc. Symp. Proc.* **1995**, *358*, 387−392.
(36) Song, J. H.; Sailor, M. J. *J. Am. Chem. Soc.* **1998**, *120*, 2376−2381.
(37) Kim, N. Y.; Laibinis, P. E. *J. Am. Chem. Soc.* **1998**, *120*, 4516−4517.
(38) Warntjes, M.; Vieillard, C.; Ozanam, F.; Chazalviel, J.-N. *J. Electrochem. Soc.* **1995**, *142*, 4138−4142.
(39) Gilman, H.; Langham, W.; Moore, F. W. *J. Am. Chem. Soc.* **1940**, *62*, 2327.
(40) Gilman, H.; Moore, F. W.; Baine, O. *J. Am. Chem. Soc.* **1941**, *63*, 2479.
(41) Higashi, G. S.; Chabal, G. W.; Trucks, G. W.; Raghavachari, K. *Appl. Phys. Lett.* **1990**, *56*, 656−658.
(42) Hassler, K.; Koll, W. *J. Organomet. Chem.* **1995**, *487*, 223−226.
(43) Wyman, D. P.; Wang, J. Y. C.; Freeman, W. R. *J. Org. Chem.* **1963**, *28*, 8, 3173−3177.
(44) Meen, R. H.; Gilman, H. *J. Org. Chem.* **1958**, *23*, 314.

(45) Rosenberg, H.; Groves, J. D.; Tamborski, C. *J. Org. Chem.* **1960**, *25*, 243.

(46) Occasionally if Mg or halide signals were seen in XPS after sonication, the surface was rinsed briefly with water and methanol and then re-characterized.

(47) Tufts, B. J.; Kumar, A.; Bansal, A.; Lewis, N. S. *J. Phys. Chem.* **1992**, *96*, 4581−4592.

(48) Grunthaner, P. J.; Grunthaner, F. J.; Fathauer, R. W.; Lin, T. L.; Hecht, M. H.; Bell, L. D.; Kaiser, W. J.; Schowengerdt, F. D.; Mazur, J. H. *Thin Solid Films* **1989**, *183*, 197.

(49) Raider, S. I.; Flitsch, R.; Palmer, M. J. *J. Electrochem. Soc.* **1975**, *122*, 413−418.

(50) Himpsel, F. J.; Meyerson, B. S.; McFeely, F. R.; Morar, J. F.; Taleb-Ibrahimi, A.; Yarmoff, J. A. Core Level Spectroscopy at Silicon Suraces and Interfaces. In *Photoemission and Absorption Spectroscopy of Solids and Interfaces with Synchrotron Radiation*; Campagna, M., Rosei, R., Eds.; North-Holland Elsevier Science Publishers B. V.: Amsterdam, 1990.

(51) Himpsel, F. J. *Acta Phys. Polon. A* **1994**, *86*, 771−785.

(52) Whitman, L. J.; Joyce, S. A.; Yarmoff, J. A.; McFeely, F. R.; Terminello, L. J. *Surf. Sci.* **1990**, *232*, 297.

(53) Seah, M. P. Quantification of AES and XPS. In *Practical Surface Analysis*, 2nd ed.; Briggs, D., Seah, M. P., Eds.; John Wiley & Sons: Chichester, 1990; Vol. 1; pp 201−255.

(54) Scofield, J. H. *J. Electron Spectrosc. Relat. Phenom.* **1976**, *8*, 129.

(55) Sconce, J. S. *Chlorine, its Manufacture, Properties and Uses.*; Reinhold Pub. Corp.: New York, 1962.

(56) Durbin, T. D.; Simpson, W. C.; Chakarian, V.; Shuh, D. K.; Varekamp, P. R.; Lo, C. W.; Yarmoff, J. A. *Surf. Sci.* **1994**, *316*, 257.

(57) Schnell, R. D.; Rieger, D.; Bogen, A.; Himpsel, F. J.; Wandelt, K.; Steinmann, W. *Phys. Rev. B* **1985**, *32*, 8057−8065.

(58) Yarmoff, J. A.; Shuh, D. K.; Durbin, T. D.; Lo, C. W.; Lapiano-Smith, D. A.; McFeely, F. R.; Himpsel, F. J. *J. Vac. Sci. Technol.* **1992**, *A10*, 2303−2307.

(59) Laibinis, P. E.; Bain, C. D.; Whitesides, G. M. *J. Phys. Chem.* **1991**, *95*, 7017−7021.

(60) Widdra, W.; Huang, C.; Yi, S. I.; Weinberg, W. H. *J. Chem. Phys.* **1996**, *105*, 5605−5617.

(61) Schulze, G.; Henzler, M. *Surf. Sci.* **1983**, *124*, 336−350.

(62) Tillman, N.; Ulman, A.; Schildkraut, J. S.; Penner, T. L. *J. Am. Chem. Soc.* **1988**, *110*, 6136−6144.

(63) In *Annual Book of ASTM Standards*; 1990; pp F 576.

(64) Chabal, Y. J.; Harris, A. L.; Raghavachari, K.; Tully, J. C. *Int. J. Mod. Phys. B* **1993**, *7*, 1031−1078.

(65) Dumas, P.; Chabal, Y. J.; Jakob, P. *Appl. Surf. Sci.* **1993**, *65/66*, 580−586.

(66) Pietsch, G. J.; Higashi, G. S.; Chabal, Y. J. *Appl. Phys. Lett.* **1994**, *64*, 3115−3117.

(67) Grunthaner, F. J.; Grunthaner, P. J.; Vasquez, R. P.; Lewis, B. F.; Maserjian, J.; Madhukar, A. *Phys. Rev. Lett.* **1979**, *43*, 1683.

(68) Grunthaner, P. J.; Hecht, M. H.; Grunthaner, F. J.; Johnson, N. M. *J. Appl. Phys.* **1987**, *61*, 629−638.

(69) Cheng, K. L. *Japan. J. Appl. Phys.* **1995**, *34*, 5527.

(70) Stinespring, C. D.; Wormhoudt, J. C. *J. Appl. Phys.* **1989**, *65*, 1733−1742.

(71) Mende, G.; Finster, J.; Flamm, D.; Schulze, D. *Surf. Sci.* **1983**, *128*, 169−175.

(72) Burrows, V. A.; Chabal, Y. J.; Higashi, G. S.; Raghavachari, K.; Christman, S. B. *Appl. Phys. Lett.* **1988**, *53*, 998−1000.

(73) Yablonovitch, E.; Allara, D. L.; Chang, C. C.; Gmitter, T.; Bright, T. B. *Phys. Rev. Lett.* **1986**, *57*, 249−252.

(74) Widdra, W.; Huang, C.; Briggs, G. A. D.; Weinberg, W. H. *J. Electron. Spec. Relat. Phenom.* **1993**, *64−5*, 129.

(75) Helms, C. R.; Strausser, Y. E.; Spicer, W. E. *Appl. Phys. Lett.* **1978**, *33*, 767−769.

(76) Briggs, D.; Seah, M. P. *Auger and X-ray Photoelectron Spectroscopy*, 2nd ed.; John Wiley & Sons: New York, 1990; Vol. 1.

(77) In the literature, the Si_{Cl} peak was also deconvoluted into its $2p_{3/2}$ and $2p_{1/2}$ components. The literature value given here corresponds to the difference between the $2p_{3/2}$ component of the Si_{Cl} peak and the $2p_{3/2}$ component of the signal from the bulk. In our data analysis, no attempt was made to deconvolute the Si_{Cl} peak into its $2p_{1/2}$ and $2p_{3/2}$ components, due to uncertainty in their area ratio and peak separation. Deconvolution of our Si_{Cl} peak into its $2p_{3/2}$ and $2p_{1/2}$ components (assuming the same area ratio and peak separation parameters as for the bulk peaks) and comparison of the peak positions of the $2p_{3/2}$ component of our Si_{Cl} peak and the $2p_{3/2}$ component of our bulk signal would result in lowering in the value of the observed difference (1.09 ± 0.09 eV) and would bring it in very close agreement with the literature value).

(78) Gao, Q.; Cheng, C. C.; Chen, P. J.; Choyke, W. J.; Yates Jr., J. T. *Thin Solid Films* **1993**, *225*, 140.

(79) Gupta, P.; Coon, P. A.; Koehler, B. G.; George, S. M. *Surf. Sci.* **1991**, *249*, 92−104.

(80) Chidsey, C. E. D.; Loiacono, D. N. *Langmuir* **1990**, *6*, 682−691.

(81) Porter, M. D.; Bright, T. B.; Allara, D. L.; Chidsey, C. E. D. *J. Am. Chem. Soc.* **1987**, *109*, 3559.

(82) Laibinis, P. E.; Whitesides, G. M.; Allara, D. L.; Tao, Y. T.; Parikh, A. N.; Nuzzo, R. G. *J. Am. Chem. Soc.* **1991**, *113*, 7152−7167.

(83) Huang, C.; Widdra, W.; Wang, X. S.; Weinberg, W. H. *J. Vac. Sci. Technol.* **1993**, *A11*, 2250−2254.

(84) Yoshinobu, J.; Tsuda, H.; Onchi, M.; Nishijima, M. *Solid State Commun.* **1986**, *60*, 801−805.

(85) Ewen, B.; Strobl, G. R.; Richter, D. *Faraday Discuss. Chem. Soc.* **1980**, *69*, 19.

(86) The very dense packing and high contact angles towards water and hexadecane that have been observed after treatment of crystalline Si surfaces with olefins in the presence of ultraviolet light or sources of free radicals presumably indicates facile surface exchange and/or mobility of surficial alkyl groups under the reported reaction conditions. These observations are especially interesting for overlayers formed on the (100)-oriented Si surface.